Signal Processing 94 (2014) 421–433

Contents lists available at ScienceDirect

Signal Processing

journal homepage: www.elsevier.com/locate/sigpro

Spectrally adapted Mercer kernels for support vector nonuniform interpolation

Carlos Figuera [a,*], Óscar Barquero-Pérez [a], José Luis Rojo-Álvarez [a], Manel Martínez-Ramón [b], Alicia Guerrero-Curieses [a], Antonio J. Caamaño [a]

[a] Department of Signal Theory and Communications, Universidad Rey Juan Carlos, C° del Molino S/N, 28943 Fuenlabrada, Madrid, Spain
[b] Department of Electrical and Computer Engineering, The University of New Mexico, Albuquerque, NM, 87101, USA

ARTICLE INFO

Article history:
Received 17 December 2012
Received in revised form
21 May 2013
Accepted 12 July 2013
Available online 20 July 2013

Keywords:
Autocorrelation kernel
Mercer kernel
Support vector regression
Nonuniform interpolation

ABSTRACT

Interpolation of nonuniformly sampled signals in the presence of noise is a widely analyzed problem in signal processing applications. Interpolators based on Support Vector Machines (SVM) with Gaussian and *sinc* Mercer kernels have been previously proposed, obtaining good performance in terms of regularization and sparseness. In this paper, inspired in the classical spectral interpretation of the Wiener filter, we explore the impact of adapting the spectrum of the SVM kernel to that of the observed signal. We provide a theoretical foundation for this approach based on a continuous-time equivalent system for interpolation. We study several kernels with different degrees of spectral adaptation to band-pass signals, namely, modulated kernels and autocorrelation kernels. The proposed algorithms are evaluated with extensive simulations with synthetic signals and an application example with real data. Our approach is compared with SVM with Gaussian and *sinc* kernels and with other well known interpolators. The SVM with autocorrelation kernel provides the highest performance in terms of signal to error ratio in several scenarios. We conclude that the estimated (or actual if known) autocorrelation of the observed sequence can be straightforwardly used as a spectrally adapted kernel, outperforming the classic SVM with low pass kernels for nonuniform interpolation.

1. Introduction

Shannon's work on uniform sampling [1,2] states that a noise-free, band-limited, uniformly sampled continuous-time signal can be perfectly recovered whenever the sampling rate is larger than or equal to twice the signal bandwidth. These initial results have been extended both in theoretical studies [3–6] and in practical applications [7–9]. However, the interpolation problem when these assumptions are not met becomes a very hard one, and many approaches have been proposed by extending Shannon's original idea.

A seminal work in this setting was Yen's algorithm [11]. In that work an expression for the uniquely defined interpolator of a nonuniformly sampled band-limited signal is computed by minimizing the energy of the reconstructed signal. The solution is given as the weighted sum of *sinc* kernels with the same bandwidth as the signal. This algorithm suffers from ill posing due to the degrees of freedom of the solution [8]. This limitation is alleviated with the inclusion of a regularization term [12]. Other interpolation algorithms using the *sinc* kernel have been proposed [8,13,14], in which the *sinc* weights are obtained according to the minimization of the maximum error on the observed data. These algorithms, which use the *sinc* kernel as their basic interpolation function, implicitly assume a band-limited signal

* Corresponding author. Tel.: +34 91 488 84 06; fax: +34 91 488 75 00.
E-mail addresses: carlos.figuera@urjc.es, cfiguera@gmail.com (C. Figuera), oscar.barquero@urjc.es (Ó. Barquero-Pérez), joseluis.rojo@urjc.es (J.L. Rojo-Álvarez), manel@tsc.uc3m.es (M. Martínez-Ramón), alicia.guerrero@urjc.es (A. Guerrero-Curieses), antonio.caamano@urjc.es (A.J. Caamaño).

0165-1684/$ - see front matter © 2013 Elsevier B.V. All rights reserved.
http://dx.doi.org/10.1016/j.sigpro.2013.07.010

to be interpolated. For non-band-limited signals, other algorithms have considered a non-band-limited kernel, such as the Gaussian kernel [5]. Finally, very efficient methods have been recently developed to reduce the computational complexity of the interpolator, for example by using filter banks [15,16], or a modified weighted version of the Lagrange interpolator [17] (see also references therein). It is interesting to note that the well-known Wiener filter has received less attention than the use of Gaussian or *sinc* kernel expansions for nonuniform-sampled signal interpolation problems [10].

On a different theoretical framework, Support Vector Machines (SVM) have been proposed in recent years as learning-from-samples tools for a number of problems, including classification and regression [18], and in many practical applications [19]. SVM algorithms have been recently proposed for nonuniform-sampled signal interpolation [20], using *sinc* and Gaussian kernels, and showing good performance for low-pass signals in terms of robustness, sparseness, and regularization capabilities. SVM algorithms have to be formulated in terms of Mercer kernels, and a well-known theoretical result is that any autocorrelation function is a valid Mercer kernel [22]. However, the suitability of using the autocorrelation of the observed process as the SVM kernel for interpolation problems has not been analyzed so far. Moreover, no previous analysis can be found on the SVM kernel choice which takes into account the spectral adaptation between the observed signal, the kernel itself, and the Lagrange multipliers yielded by the model.

In this work, we propose the use of SVM algorithms to solve the nonuniform sampling interpolation problem by exploring several Mercer kernels that are spectrally adapted to the signal to be interpolated. To accomplish this task, we first analyze the relationship between the Wiener filter and the SVM algorithm for this problem, using the spectral interpretation of both algorithms. Then, according to this analysis, we examine different SVM interpolation kernels accounting for different degrees of spectral adaptation and performance, namely, band-pass kernels, estimated signal autocorrelation kernels, and actual signal autocorrelation kernels. A preliminary version of this work has been presented in [23].

The paper is organized as follows. Section 2 reviews several interpolation algorithms, including the Wiener filter, the Yen algorithm, and the SVM interpolator, and summarizes their well-known spectral interpretation. In Section 3, a continuous time equivalent model for the SVM interpolation allows us to propose a list of kernels for SVM interpolation with different degrees of spectral adaptation. Section 4 includes a set of experiments evaluating the importance of this spectral adaptation, and comparing the performance of several interpolation algorithms and their robustness with non-Gaussian noise and nonuniform sampling in synthetic data and in an application example. Section 5 provides a concluding summary.

2. Algorithms for nonuniform interpolation

In this section, we first briefly introduce notation and define the problem to be solved. Second, three nonuniform interpolation algorithms, namely, Wiener filter [10], Yen regularized interpolator [11,12], and SVM interpolator [20] are described. Although much more interpolation methods have already been proposed in the literature, we limit ourselves to these three cases for two reasons: (i) they are representative cases of optimal algorithms (with a different optimality concept for each case), and (ii) they have a straightforward spectral interpretation, which allows an interesting comparison with the algorithms proposed in this work.

Let $x(t)$ be a continuous-time signal with finite-energy, consisting of a possibly band-limited signal $z(t)$, which can be seen as a realization of a random process, corrupted with additive noise $w(t)$, *i.e.* $x(t)=z(t)+w(t)$, where the noise is modeled as a zero-mean Wide Sense Stationary (WSS) process. This signal has been observed on a set of N unevenly spaced time instants, $\{t_n,\ n=1,\ldots,N\}$, obtaining the set of observations $\boldsymbol{x}=[x(t_1),\ldots,x(t_n),\ldots,x(t_N)]^T$.

Then, the nonuniform interpolation problem consists in finding a continuous-time signal $\hat{z}(t)$ that approximates the noise-free interpolated signal in a set of K time instants, $\{t'_k,\ k=1,\ldots,K\}$.

2.1. Wiener filter for nonuniform interpolation

Time domain analysis: As described in [10], a Bayesian approach to solve this problem amounts to the Wiener filter [24]. Assuming that $z(t)$ is zero mean, the linear estimator is given by

$$\hat{z}(t'_k)=\boldsymbol{a}_k^T\boldsymbol{x} \quad \text{for } k=1,\ldots,K \tag{1}$$

The scalar Linear Minimum Mean Square Error (LMMSE) estimator is obtained when $\boldsymbol{a}_k$ is chosen to minimize the MSE and takes the following form [10]:

$$\hat{z}(t'_k)=\boldsymbol{r}_{z_k}^T\boldsymbol{C}_{xx}^{-1}\boldsymbol{x} \quad \text{for } k=1,\ldots,K \tag{2}$$

Vector $\boldsymbol{r}_{z_k}$ contains the cross covariance values between the observed signal and the signal interpolated at time t'_k, that is $\boldsymbol{r}_{z_k}=[r_{zz}(t'_k-t_1),\ldots,r_{zz}(t'_k-t_N)]^T$, where $r_{zz}(\tau)$ is the autocorrelation of the *noise-free* signal for a time shift τ. $\boldsymbol{C}_{xx}$ is the covariance matrix of the observations and, assuming WSS data with zero mean, it is computed as $\boldsymbol{C}_{xx}=\boldsymbol{R}_{zz}+\boldsymbol{R}_{ww}$, where $\boldsymbol{R}_{zz}$ is the autocovariance matrix of the signal with components i,j given by $\boldsymbol{R}_{zz}(i,j)=r_{zz}(t_i-t_j)$, and $\boldsymbol{R}_{ww}$ is the noise covariance matrix. For the *i.i.d.* case, $\boldsymbol{R}_{ww}=\sigma_w^2\boldsymbol{I}_N$, with σ_w^2 the noise power and $\boldsymbol{I}_N$ the identity matrix of size $N\times N$. Thus, $\hat{z}(t'_k)$ is given by

$$\hat{z}(t'_k)=[(\boldsymbol{R}_{zz}+\sigma_w^2\boldsymbol{I}_N)^{-1}\boldsymbol{r}_{z_k}]^T\boldsymbol{x} \tag{3}$$

Although the solution in (3) is optimal in the MSE sense, two main drawbacks can arise when using it for practical applications: (1) it implies the inversion of a matrix that, specially for high Signal to Noise Ratio (SNR), can be almost singular, so the problem can become numerically ill-posed; and (2) the knowledge of the autocorrelation of the signal $r_{zz}(\tau)$ at every $\tau=t_i-t_j$ is needed, so it must be estimated from the observed samples if it is not known.

Frequency domain analysis: The solution of the LMMSE estimator given by (2) can be seen as the convolution of the observations with a filter with impulse response $h_W^{(k)}[n]=a[k-n]$. For a finite number of nonuniform samples,

the solution cannot be converted into a time-invariant filter since it depends on k index, which is a significant different with the uniform-sampling case. However, in order to provide a simple spectral interpretation of the interpolator we assume that $N\to\infty$ and then (3) can be approximated as the convolution of the observations with a time-invariant filter with response $h_W[n]$, which does not depend on the time index k [10],

$$\hat{z}(t'_k)=\sum_{n=-\infty}^{\infty} h_W[n]x(t_k-t_n) \tag{4}$$

In this case, the coefficients of the filter $h_W[n]$ can be computed using the Wiener–Hopf equations [24]. By applying the Fourier transform to these equations, the transfer function of the filter is finally obtained:

$$H_W(f)=\frac{P_{zz}(f)}{P_{zz}(f)+P_{ww}(f)}=\frac{\eta(f)}{\eta(f)+1} \tag{5}$$

where $P_{zz}(f)$ and $P_{ww}(f)$ are the Power Spectral Density (PSD) of the original signal and the noise respectively, and $\eta=P_{zz}(f)/P_{ww}(f)$ represents the local Signal to Noise Ratio (SNR) in a frequency f. Obviously, $0<H_W(f)<1$, tending to 1 (to 0) in spectral bands with high (low) SNR. Hence, the Wiener filter enhances (attenuates) the signal in those bands with high (low) SNR, and the autocorrelation of the process to be interpolated is a natural indicator of the relevance of each spectral band in terms of SNR.

2.2. Yen regularized interpolator

Time domain analysis: Inspired by Shannon's sampling theorem, *a priori* information can be used for band-limited signal interpolation by means of a *sinc* kernel. In this case, the signal is modeled with a *sinc* kernel expansion as

$$x(t'_k)=z(t'_k)+w(t'_k)=\boldsymbol{a}^T\boldsymbol{s}_k+w(t'_k)\quad \text{for } k=1,\ldots,K \tag{6}$$

with $\boldsymbol{s}_k$ an $N\times 1$ column vector with components $\boldsymbol{s}_k[n]=sinc(\sigma_0(t'_k-t_n))$, where $sinc(t)=\sin(t)/t$ and parameter $\sigma_0=\pi/T_0$ is the *sinc* function bandwidth. Then, the interpolator can be stated as follows:

$$\hat{z}(t'_k)=\boldsymbol{a}^T\boldsymbol{s}_k\quad \text{for } k=1,\ldots,K \tag{7}$$

When Least Squares (LS) strategy is used to estimate $\boldsymbol{a}$, Yen's solution [11, Theorem IV] is obtained. If a regularization term is used to prevent numerical ill-posing, $\boldsymbol{a}$ is obtained by minimizing

$$\mathcal{L}_{reg}=\frac{1}{2}\|\boldsymbol{x}-\boldsymbol{S}\boldsymbol{a}\|^2+\frac{\delta}{2}\|\boldsymbol{a}\|^2 \tag{8}$$

where $\boldsymbol{S}$ is a square matrix with elements $\boldsymbol{S}(n,k)=sinc(\sigma_0(t_n-t'_k))$, and δ tunes the trade-off between solution smoothness and the errors in the observed data. In this case, $\boldsymbol{a}$ is given by

$$\boldsymbol{a}=(\boldsymbol{S}^2+\delta\boldsymbol{I}_N)^{-1}\boldsymbol{S}\boldsymbol{x} \tag{9}$$

The use of the regularization term leads to solutions that are suboptimal in the MSE sense.

Frequency domain analysis: An asymptotic analysis similar to the one presented for the Wiener filter can be done based on (9) and (7). Using a continuous time equivalent model for the interpolation algorithm (see Section 3 for further details) the interpolation algorithm can be interpreted as a filtering process over the input signal, this is

$$\hat{z}(t)=h_Y(t)*x(t) \tag{10}$$

where $*$ denotes the convolution operator. Now, the transfer function of the filter is given by

$$H_Y(f)=\frac{P_{ss}(f)}{P_{ss}(f)+\delta} \tag{11}$$

where $P_{ss}(f)$ is the PSD of $sinc(\sigma_0 t)$ (since this one is deterministic, $P_{ss}(f)\equiv|S(f)|^2$ with $S(f)$ the Fourier transform of the *sinc* function), which is a rectangular pulse of width σ_0. $H_Y(f)$ takes the value $1/(1+\delta)$ inside the passband of $P_{ss}(f)$ and 0 outside. Therefore, if σ_0 is equal to the signal bandwidth, the filter attenuates the noise outside the signal band and does not affect the components inside the band. A comparison between (11) and (5) reveals that both interpolators can be interpreted as filters in the frequency domain, but in the case of Yen's algorithm the local SNR $\eta(f)$ is approximated by the *sinc* kernel PSD, $P_{ss}(f)$.

2.3. SVM interpolation

An alternative to the use of LS criterion in nonuniform interpolation is the SVM approach [25]. We next summarize the procedure presented in [20], in order to use the most relevant results in the next section.

Let us assume a nonuniform interpolator of the form

$$\hat{z}(t'_k)=\boldsymbol{a}^T\boldsymbol{\varphi}(t'_k) \tag{12}$$

where $\boldsymbol{a}$ is an $N\times 1$ weight vector which defines the solution and $\boldsymbol{\varphi}(t'_k)$ is a nonlinear transformation of the time instants to a Hilbert space $\mathcal{H}$, provided with a dot product

$$\boldsymbol{\varphi}(t_1)^T\boldsymbol{\varphi}(t_2)=K(t_1,t_2) \tag{13}$$

with $K(\cdot,\cdot)$ being a kernel that satisfies Mercer's Theorem [18]. The solution of the SVM is stated in terms of dot products of the transformed input samples. Hence, (13) indicates that the nonlinear transformation in (12) will be done implicitly by means of a kernel function.

In order to construct the interpolator, vector $\boldsymbol{a}$ must be found. For this purpose, following the structural risk minimization principle, a cost function on the errors in the sampling instants plus a regularization term should be minimized [18]. In this work, a ε-Huber cost [26] function is used:

$$\mathcal{L}_{\varepsilon H}(e_n)=\begin{cases}0, & |e_n|<\varepsilon\\ \dfrac{1}{2\gamma}(|e_n|-\varepsilon)^2, & \varepsilon\le|e_n|<\varepsilon+\gamma C\\ C(|e_n|-\varepsilon)-\dfrac{1}{2}\gamma C^2, & |e_n|\ge\varepsilon+\gamma C\end{cases} \tag{14}$$

where $e_n=x(t_n)-\hat{z}(t_n)$, and ε, γ and C are free parameters to be adjusted using *a priori* knowledge (see [21] for further details). Using this cost function, the primal functional to be optimized in order to obtain $\boldsymbol{a}$ is

$$\mathcal{L}_p=\frac{1}{2}\|\boldsymbol{a}\|^2+\frac{1}{2\gamma}\sum_{n\in I_1}(\xi_n^2+\xi_n^{*2})+C\sum_{n\in I_2}(\xi_n+\xi_n^*)-\sum_{n\in I_2}\frac{\gamma C^2}{2} \tag{15}$$

subject to the constraints

$$x_n - \boldsymbol{a}^T\boldsymbol{\varphi}(t_n) \le \varepsilon + \xi_n$$
$$-x_n + \boldsymbol{a}^T\boldsymbol{\varphi}(t_n) \le \varepsilon + \xi_n^* \tag{16}$$

where $\xi_n^{(*)} = \max\{0, |e_n| - \varepsilon\}$ are the error magnitude outside the insensitivity region for positive and negative errors, and sets $\mathcal{I}_1$ and $\mathcal{I}_2$ contains the indices of errors that lie in the quadratic and linear sections of the cost function, respectively [26].

The SVM approach allows to control the estimator smoothness through the first term of (15). Also, due to the insensitivity region of the cost function the solution is sparse, meaning that only a subset of the original signal samples are used for building the solution, and hence the computational burden of the interpolator is reduced. Finally, the cost function approaches maximum likelihood (ML) for Gaussian noise and is robust against non-Gaussian interferences as impulsive noise [26].

Using the Lagrange method for solving the problem in (15) and (16), the solution is

$$\boldsymbol{a} = \sum_{n=1}^{N} (\alpha_n - \alpha_n^*)\boldsymbol{\varphi}(t_n) = \sum_{n=1}^{N} \beta_n \boldsymbol{\varphi}(t_n) \tag{17}$$

where $\beta_n = \alpha_n - \alpha_n^*$ are the Lagrange multipliers for constraints in (16) [20]. Finally, by combining (12) and (17), and expanding the scalar product into a summation, the interpolated signal is given by

$$\hat{z}(t'_k) = \sum_{n=1}^{N} \beta_n \boldsymbol{\varphi}(t_n)^T \boldsymbol{\varphi}(t'_k) = \sum_{n=1}^{N} \beta_n K(t_n, t'_k)$$
$$= \sum_{n=1}^{N} \beta_n K(t_n - t'_k). \tag{18}$$

where for the last equality we have assumed that the kernel fulfills the condition $K(x,y) = K(x-y)$. In that case, the kernel can be thought as a time-invariant system that provides a convolutional model for the solution [27]. Conversely, it is known that for a function $K(\cdot,\cdot)$ to be a valid shift invariant kernel, it is a necessary and sufficient condition that it has a nonnegative Fourier transform [28].

2.4. Some comparative remarks

It can be seen that both Yen and Wiener filter algorithms use the LS (regularized for Yen method) criterion. However, Wiener algorithm is linear with the observations, and it does not assume any *a priori* decomposition of the signal in terms of building functions. Instead, it relies on the knowledge of the autocorrelation function, which can be hard to be estimated in a number of applications. Alternatively, Yen algorithm is nonlinear with respect to the observations and assumes an *a priori* model based on *sinc* kernels. Hence, the knowledge of the signal autocorrelation is not needed. The SVM interpolation uses a different optimization criterion, which is the structural risk minimization, and its solution is nonlinear with respect to the observations since it assumes a signal decomposition in terms of a given Mercer kernel.

3. Spectrally adapted Mercer kernels

In this section, we present a Continuous-time Equivalent System for Nonuniform Interpolation (CESNI), which represents the solution of the interpolation problem based on the SVM approach. The objective of presenting a continuous-time equivalent system is to establish a frequency domain description of the interpolation SVM algorithm. Based on the analysis of the CESNI model, several effective Mercer kernels are proposed for SVM-based nonuniform sampling interpolation. These kernels account for different degrees of spectral adaptation to the observed data.

Definition 1 (*CESNI*). Given the SVM procedure described in Section 2.3, we define its continuous-time equivalent system as

$$\hat{z}(t) = \mathcal{T}\{x(t)\} \tag{19}$$

with $x(t) = z(t) + w(t)$, $\hat{z}(t)$ the estimation of $z(t)$, and $\mathcal{T}\{\cdot\}$ a continuous time nonlinear feedback system. If $\mathcal{T}\{\cdot\}$ is evaluated in a set of N time instants $\{t_n,\ n = 1,\ldots,N\}$ taken from a uniform random distribution, the system defined by the solution in Section 2.3 is obtained.

In order to define $\mathcal{T}\{\cdot\}$, recall that Lagrange coefficients are related with the observed data by the derivative of the cost function, *i.e.* $\beta_n = \mathcal{L}_{\varepsilon H}'(e_n) \equiv d\mathcal{L}_{\varepsilon H}(e_n)/de$ (proof can be found in [21]) and that $e_n = x(t_n) - \hat{z}(t_n)$. Using these results, it can be seen that the solution defined in (18) can be modeled as a feedback system, and we will define $\mathcal{T}\{\cdot\}$ as its continuous time version, which is represented in Fig. 1. CESNI elements are subsequently scrutinized.

Property 1 (*Residual continuous time signal*). *Given the CESNI of SVM algorithm for unidimensional signal interpolation, the residual continuous time signal is given by*

$$e(t) = x(t) - \hat{z}(t) \tag{20}$$

and it corresponds to the continuous time signal from which the residuals are sampled.

Property 2 (*Model coefficient continuous-time signal*). *In the CESNI of SVM algorithm for unidimensional signal interpolation, the Model Coefficient Continuous-time Signal is given by the following set of equations*:

$$\beta_e(t) = \mathcal{L}'_{\varepsilon H}(e(t)) \tag{21}$$

$$s(t) = \sum_{n=1}^{N} \delta(t_n) \tag{22}$$

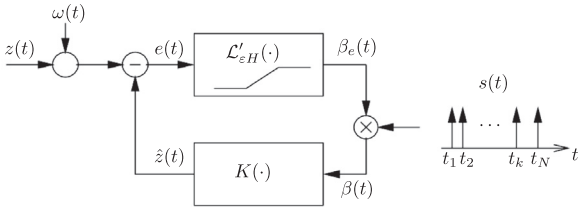

Fig. 1. CESNI for the SVM interpolation algorithm. The interpolated signal $\hat{z}(t)$ is built by filtering the continuous-time sampled version of the Lagrange coefficients $\beta(t)$ with the SVM kernel $K(t)$.

$$\beta(t) = \beta_e(t) \times s(t) = \sum_{n=1}^{N} \beta_n \delta(t_n) \tag{23}$$

where $\beta_e(t)$ is the equivalent continuous signal for the Lagrange coefficient sequence, $\beta(t)$ is its sampled version, and $\delta(t)$ represents Dirac's delta function. Hence (23) represents the discrete set of the model coefficients given by the SVM algorithm as obtained by random sampling of a continuous time signal $\beta_e(t)$.

Property 3 (*Recovered continuous-time signal*). *In the CESNI of SVM algorithm for unidimensional signal interpolation, the recovered continuous-time signal is given by*

$$\hat{z}(t) = K(t) * \beta(t) \tag{24}$$

which shows that the kernel works as a linear, time-invariant filter and that the Lagrange coefficients are the inputs to that filter.

Consequently, denoting the PSD of $\hat{z}(t)$, $K(t)$, and $\beta(t)$ as $P_{\hat{Z}}(f)$, $P_{\mathcal{K}}(f)$, and $P_{\mathcal{B}}(f)$, respectively, the recovered signal PSD is given by $P_{\hat{Z}}(f) = P_{\mathcal{K}}(f)P_{\mathcal{B}}(f)$, and hence we can conclude that the kernel is shaping the output in the frequency domain. On the one hand, an appropriate adaptation of the kernel spectrum to the one of the original signal shall improve the interpolation performance. On the other hand, if the signal and kernel spectra are not in the same band, the performance shall be really poor. This would be the case of the *sinc* or the Gaussian kernels when used for band-pass signal interpolation. This suggests that Mercer kernels represent the transfer function which should emphasize the recovered signal in those bands with higher SNR. Looking at the Wiener filter transfer function in (5) we can see that the signal autocorrelation could be used for this purpose, since its Fourier transform is the PSD of the signal.

Nevertheless, despite these are well known principles of signal processing, little attention has been paid to the possibility of using spectrally adapted Mercer kernels in SVM-based interpolation algorithms. According to these considerations, we now propose several Mercer kernels with different degrees of spectral adaptation, namely, modulated and autocorrelation kernels.

Property 4 (*Modulated kernels*). *If $z(t)$ is a band-pass signal centered at f_0, modulated versions of RBF and sinc kernels given by*

$$K(t_n, t'_k) = sinc(\sigma_0(t_n - t'_k)) \sin(2\pi f_0(t_n - t'_k)) \tag{25}$$

$$K(t_n, t'_k) = \exp\left(-\frac{(t_n - t'_k)^2}{2\sigma_0^2}\right) \sin(2\pi f_0(t_n - t'_k)) \tag{26}$$

are suitable Mercer kernels. Moreover, their spectra are adapted to the signal spectrum. Note that in this case, an additional free parameter ω_0 has to be settled for the kernel.

Property 5 (*Autocorrelation kernels*). *Similar to the Wiener filter, the autocorrelation of the signal to be interpolated ($z(t)$) or its noisy observations ($x(t_n)$) can be used to define the following kernels*:

$$K_{ideal}(t_n, t'_k) = r_{zz}(t_n - t'_k) \tag{27}$$

$$K_{est}(t_n, t'_k) = r_{xx}(t_n - t'_k) \tag{28}$$

which are the ideal (actual) autocorrelation function computed from the underlying process and autocorrelation function estimated from the observations, respectively.

If the second order statistics of the process are known, kernel defined in (27) can be used. When the autocorrelation of the process is not known, an estimation procedure must be used. Note that this problem is not exclusive of the SVM interpolator, but is also present in the Wiener case. However, as shown in the experiments, due to the robustness of the SVM algorithm, simple procedures for estimating the autocorrelation functions can be used.

Fig. 2 illustrates the effect of using different kernels. The signal to be interpolated is band-pass, so its interpolation

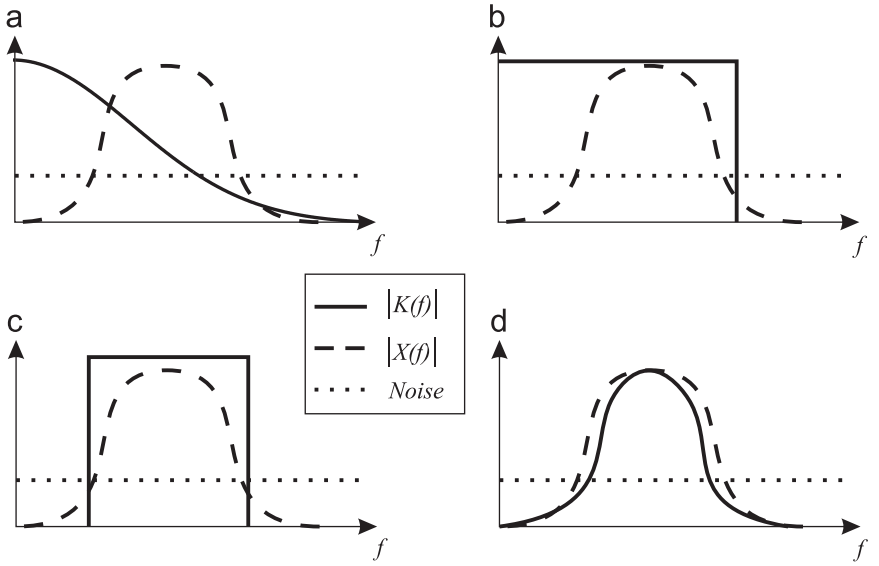

Fig. 2. Illustration of the spectral adaptation of the kernels to the observations for a band-pass signal: (a) with RBF kernel, (b) with *sinc* kernel, (c) with modulated *sinc* kernel, and (d) with autocorrelation kernel.

with low-pass kernels, either RBF (a) or *sinc* (b), can be a loose spectral adaptation which indeed emphasizes the noise in the low-pass band. In (c), the use of a modulated band-pass *sinc* kernel allows us to enhance the transfer function spectral adaptation to the signal spectral profile, which is further refined in (d) when using the estimated autocorrelation as interpolation kernel.

4. Experiments

In this section, the described algorithms are experimentally assessed. We first analyze their performance when interpolating a band-pass signal. Then, we evaluate the interpolation of two signals with very different spectra, to assess the impact of the kernel spectral adaptation. We also test different levels of nonuniformity in the sampling process, different numbers of training samples, and non-Gaussian noise. In a second set of experiments, we test the algorithms with several one-dimensional functions with different and representative spectral profiles. Finally, the applicability of SVM algorithms is illustrated by interpolating a set of Heart Rate Variability (HRV) signals, which are nonuniformly sampled time series.

4.1. Experimental setup

We benchmarked the interpolation algorithms that are summarized in Table 1, including all the methods described above and the functionally weighted version of the Lagrange interpolator described in [17].

For *Wien* and *SVM-Corr* algorithms the autocorrelation function had to be estimated from the observed samples. Note that the autocorrelation had to be computed for every time shift $\tau = t_n - t'_k$, so it had to be estimated over a grid with a resolution much higher than that of the observed samples. Hence, two steps might be carried out: (1) estimating the autocorrelation from the observed samples and (2) interpolating it for every time shift $\tau = t_n - t'_k$. Although many methods exist for this purpose, we propose to use a simple procedure based on frequency-domain interpolation. The main reason for this choice is that the overall procedure is simple and well-established. Specifically, the method consists of (1) a Lomb Periodogram to estimate the PSD of the signal [29], and (2) a zero padding technique in the frequency domain to carry out the interpolation step. Finally, inverse Fourier transform of the zero padded PSD was used for computing the autocorrelation function.

Table 1
List of algorithms benchmarked in the experiments.

Algorithm description	Label
Yen algorithm with regularization	*Yen*
Weighted Lagrange interpolator	*WLI*
Wiener filter with estimated autocorrelation	*Wien*
Wiener filter with actual (ideal) autocorrelation	*Wien-Id*
SVM with low-pass RBF kernel	*SVM-RBF*
SVM with low-pass *sinc* kernel	*SVM-Sinc*
SVM with estimated autocorrelation kernel	*SVM-Corr*
SVM with actual (ideal) autocorrelation kernel	*SVM-CorrId*

For the synthetic experiments, a one-dimensional signal with spectral information contained in $[-B/2, B/2]$ was interpolated. This signal was sampled in a set of L unevenly time instants, different for each realization, with an average sampling interval T, such that $BT=1$. The interpolation instants lied on a uniform grid with step $T_{int} = T/F$, with F the interpolation factor. The nonuniform sampling time instants were simulated by adding a random quantity taken from a uniform distribution in the range $[-u, u]$ to the equally spaced time instants $t_k = kT,\ k = 1, 2, \ldots, L$. In order to simplify the computation of the kernels, each time instant was rounded to be a multiple of T_{int}. The performance of each algorithm was measured by using the S/E indicator, that is, the ratio between the power of the signal and the power of the error in dB. Each experiment was repeated 50 times.

4.2. Interpolation of band-pass signals

To get a first insight of the impact of the kernel spectral adaptation on the algorithms performance, we compared them when interpolating a test signal consisting of a modulated squared *sinc* function (MSSF), defined by

$$f(t) = sinc^2\left(\frac{\pi}{T_0}t\right)\cos\left(2\pi f_1 t\right) \tag{29}$$

where T_0 and f_1 are chosen in order that the signal bandwidth fulfills $BT=1$. The spectrum of this signal is a triangle centered at f_1. The experiment was carried out with $L=32$ samples, $T=0.5$ s, a nonuniformity parameter $u = T/10$, and for Gaussian noise with different values of SNR. Fig. 3 shows the spectra of the original and reconstructed signals and the error of reconstruction of the Yen and the SVM algorithms. The error at low frequencies (where there is no significant signal power) is high for the SVM with low-pass kernels, since in this band the noise is enhanced by the kernel spectrum. On the contrary, it can be seen that the error produced by the autocorrelation kernel is quite lower, since it is adapted to the signal spectrum.

Table 2 represents the performance of all the algorithms for different SNRs. It can be observed that both SVM-CorrId and Wien-Id methods, which are based on the perfect knowledge of the signal autocorrelation, clearly outperform the other algorithms. Although the solution presented in (3) is optimal in the MSE sense, it suffers from numerical ill-posing due to the inversion of the correlation matrix, which usually presents a very high condition number. The SVM with estimated autocorrelation kernels also has a good performance, only 1 to 2 dB lower than the ideal version. Note that it clearly outperforms the non-ideal version of the Wiener filter. WLI algorithm provides intermediate S/E values, although it computational complexity is the lowest one. Finally, SVM with low pass kernels and Yen algorithms provide a performance lower than that of the others.

4.3. Spectral adaptation of SVM kernel

In order to investigate the importance of the spectral adaptation of the kernel, we analyzed the performance

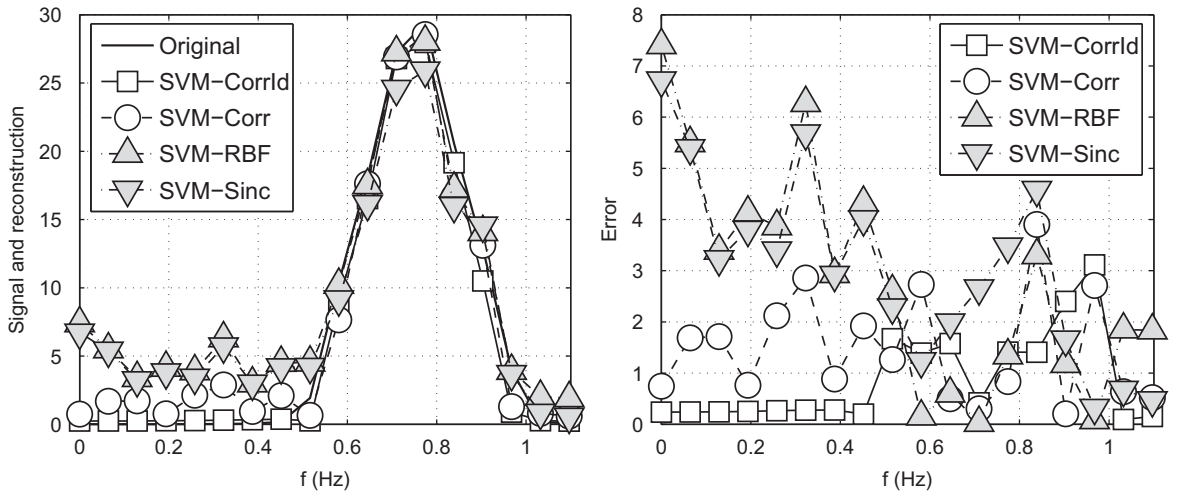

Fig. 3. Example of the spectra of the original and reconstructed signals (left) and the error of the reconstructions (right) for the modulated *sinc* squared function. $T=0.5$ s, $L=32$, SNR$=10$ dB and $u=T/10$.

Table 2
Mean S/E and (std) with SNR for a band-pass signal interpolation, $T=0.5$ s, $L=32$ and $u=T/10$. Two best in bold.

Alg.	40 dB	30 dB	20 dB	10 dB
Yen	35.1 (0.5)	29.3 (0.9)	20.3 (1.1)	10.4 (1.3)
Wien	39.8 (1.2)	30.0 (1.0)	20.2 (1.1)	10.1 (1.3)
WLI	38.4 (2.4)	29.4 (1.2)	20.1 (1.3)	10.0 (1.4)
Wien-Id	**41.2** (**1.2**)	**32.3** (**1.4**)	**22.6** (**1.7**)	**13.1** (**1.8**)
SVM-Corr	39.5 (1.9)	30.9 (1.4)	22.0 (1.3)	12.6 (1.6)
SVM-CorrId	**41.7** (**1.4**)	**32.9** (**1.4**)	**23.5** (**1.6**)	**14.9** (**1.6**)
SVM-RBF	27.4 (1.0)	26.1 (0.7)	19.2 (0.7)	10.8 (1.2)
SVM-Sinc	34.1 (0.7)	28.9 (1.1)	20.2 (1.1)	10.9 (1.2)

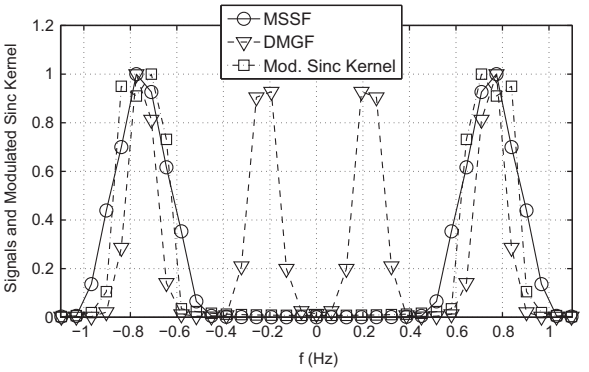

Fig. 4. Spectrum for the MSSF, DMGF and modulated *sinc* kernel.

of two SVM-based interpolators on two additional test signals. The first signal was the MSSF described in (29), whereas the second signal consisted of two Gaussian functions modulated at different frequencies and added together (labeled DMGF, from double modulated Gaussian function) given by

$$f(t)=\frac{1}{\sigma\sqrt{2\pi}}\exp\left(-\frac{t-\mu}{2\sigma^2}\right)\{\cos(2\pi f_1 t)+\cos(2\pi f_2 t)\} \qquad (30)$$

with $\sigma=3$, $f_1=0.75$ Hz and $f_2=0.25$ Hz. Following the same setup as in the previous experiments, we interpolated these two functions by using two SVM algorithms, one with the ideal autocorrelation kernel, and the other with the modulated *sinc* band-pass kernel (SVM-ModSinc) given by Eq. (25), where σ_0 and w_0 have been chosen to obtain the same spectrum as the one of the MSSF. In Fig. 4 the spectra of both functions and the modulated *sinc* kernel are shown. It can be seen that the modulated *sinc* kernel is spectrally adapted to the MSSF, but not to the DMGF. Fig. 5 shows the S/E performance for both algorithms when interpolating both functions. The modulated *sinc* kernel performs well for the MSSF, since the spectrum is similar, but the performance degrades for the DMGF.

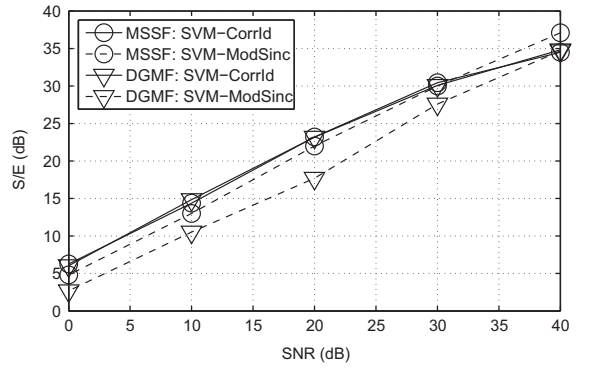

Fig. 5. S/E ratio for SVM-CorrId (solid lines) and SVM-ModSinc (dashed lines) algorithms when interpolating MSSF (circles) and DMGF (triangles). $T=0.5$ s, $L=32$, $u=T/10$.

Notably, the autocorrelation kernel is able to adapt its spectrum to both signals, and therefore it performs well with both of them.

4.4. Effect of the sampling process and the noise

4.4.1. Nonuniform sampling

Now, we examine the effect of increasing the nonuniformity parameter u from very small values to half of the sampling period. The sampling for u very small is almost uniform, while with $u=T/2$ the samples can be placed at any time instant. For this purpose, we used the MSSF and a set of logarithmically spaced values for u, from 0.001 to $T/2$, using $SNR=20$dB, and with the rest of the parameters as in Section 4.2.

Fig. 6 shows the mean and standard deviation of the S/E for all the algorithms for each value of u. *SVM-CorrId* is the most robust algorithm with respect to the nonuniform sampling. When u takes its maximum value, the difference between the *SVM-CorrId* and the rest of the algorithms is also maximal and rises up to 5 dB. Interestingly, *Wien-Id* behaves similar to *SVM-CorrId* for low values of u, which was the expected behavior since both of them use the same prior knowledge about the second order statistics of the signal. However, when u exceeds 10^{-2}, the performance of the Wiener filter degrades fast, which can be explained by the loss of stationarity caused by the nonuniform sampling. The robust nature of SVM interpolation is not affected in the same manner by this effect. Finally, SVM-Corr algorithm shows an intermediate performance, between SVM-CorrId and the rest of the algorithms.

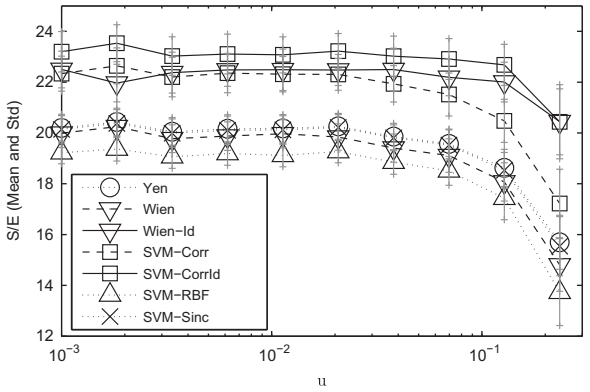

Fig. 6. S/E ratio for different values of the nonuniformity parameter (u) SNR=20 dB, T=0.5 s, L=32.

Table 3
Mean S/E and (std) with the number of samples L, for a band-pass signal interpolation, and $u=T/10$. Two best in bold.

Alg.	L=32	L=64	L=128
Yen	19.6 (0.9)	19.6 (0.8)	15.7 (2.1)
Wien	19.2 (1.0)	19.6 (0.9)	19.9 (0.5)
Wien-Id	**22.4** (**3.4**)	**22.5** (**2.9**)	**22.9** (**2.3**)
SVM-Corr	21.9 (1.2)	21.9 (0.9)	21.8 (0.8)
SVM-CorrId	**23.3** (**1.2**)	**23.2** (**1.0**)	**23.4** (**0.7**)
SVM-RBF	19.2 (1.0)	19.0 (0.8)	18.9 (0.5)
SVM-Sinc	19.5 (1.0)	19.8 (0.7)	19.5 (0.5)

4.4.2. Number of samples

In this experiment we investigated the performance of all the algorithms for different numbers of samples, using the same function and parameters as in the previous sections. Note that if the function bandwidth is not changed, the comparison would be unfair. Hence, we increased it accordingly to the number of samples. Table 3 shows the results for different lengths of the training set. Most algorithms perform similarly for all the values of L. However, Yen algorithm has a poorer behavior, since the numerical problems associated with the matrix inversion become more patent.

4.4.3. Robustness against impulse noise

SVM algorithms have shown good performance when impulse noise is present at the data [20]. We tested all the proposed algorithms with this noise, which was generated with the Bernoulli–Gaussian (BG) function $n_n^{BG}=v_n\lambda_n$ where v_n is a random process with Gaussian distribution and power σ_{BG}^2 and where λ_n is a random process which takes the value 1 with probability p and the value 0 with probability $1-p$. A value of $p=0.1$ was considered. In order to compare the robustness of each algorithm when this type of noise was present, we used the signal to impulse noise ratio (SIR) indicator, defined by

$$SIR_{dB}=10\log_{10}\left(\frac{E\{x_n-n_n^G-n_n^{BG}\}}{\sigma_{BG}^2}\right) \tag{31}$$

Table 4 shows the performance (in terms of S/E) of the proposed algorithms for different values of SIR, $SNR=10$ dB, and the rest of the parameters as in Section 4.2. In this case, due to the inherent robustness to outliers of the SVM formulation, all the SVM algorithms are robust against impulse noise, while the performance of the two Wiener filter algorithms degrades for very low SIR, hence confirming the superiority of the SVM-based solution in the case of non-Gaussian noise. Again, *SVM-CorrId* provides the best results for all SIR values, and hence shows an interesting robustness with different types of noise.

Table 4
Mean S/E and (std) with SIR (SNR=10 dB) for a band-pass signal interpolation, and $u=T/10$. Two best in bold.

Alg.	20 dB	15 dB	10 dB	5 dB	0 dB	−5 dB
Yen	10.5 (1.3)	10.2 (1.2)	9.9 (1.1)	8.7 (1.5)	6.8 (2.0)	4.5 (2.7)
Wien	10.0 (1.3)	9.8 (1.2)	9.3 (1.2)	7.9 (1.6)	5.7 (2.2)	2.9 (3.3)
Wien-Id	**13.3** (**1.8**)	**13.1** (**1.8**)	**12.9** (**1.7**)	**12.0** (**1.9**)	**10.0** (**2.3**)	**8.8** (**3.5**)
SVM-Corr	12.6 (1.6)	12.1 (1.3)	11.9 (1.5)	10.6 (1.8)	8.2 (2.7)	5.7 (3.1)
SVM-CorrId	**14.5** (**1.8**)	**14.3** (**1.4**)	**14.1** (**1.6**)	**13.0** (**2.1**)	**10.9** (**2.3**)	**10.0** (**2.7**)
SVM-RBF	10.6 (1.2)	10.3 (1.3)	10.1 (1.2)	8.9 (1.6)	6.6 (2.0)	4.4 (2.8)
SVM-Sinc	11.0 (1.1)	10.7 (1.2)	10.7 (1.2)	9.6 (1.5)	7.5 (2.1)	5.3 (2.5)

4.5. Performance for different type of signals

In this experiment we tested the performance of the analyzed algorithms with a database of functions with different kinds of spectrum. Fig. 7 shows the spectra of the nine functions which have been used for this purpose. In this case, the number of samples is $L=64$, with $T=0.24$ s and $u=T/10$. The noise was Gaussian with $SNR=10$ dB. Table 5 shows the mean S/E and its standard deviation in brackets. *SVM-CorrId* with the ideal autocorrelation kernel performs well in all the cases, followed by *SVM-Corr* most of the times. In the case of the chirp function, the *SVM-Sinc* behaves better than the *SVM-Corr*, since its spectrum is similar to the one of that function. However, the performance of this algorithm degrades for other functions (like PST or POL). Based on these results, we can conclude that the SVM with autocorrelation kernels have very good performance independently of the signal spectrum, since they are able to adapt the kernel spectra.

4.6. Interpolation of heart rate variability signals

4.6.1. Introduction

Heart rate variability (HRV) is a relevant marker of the autonomic nervous system (ANS) control on the heart. This marker has been proposed for risk stratification of lethal arrhythmias after acute myocardial infarction, as well as for prognosis of sudden death events [30]. When analyzing the HRV time series, the sequence of time intervals between two consecutive beats (called RR-Interval time series) is often used, which is by nature sampled at unevenly spaced time instants. Advanced methods for spectral analysis have shown that the HRV signal contains well defined oscillations that account for different physiological information. The spectrum of the HRV could be divided into three bands: very low frequency (VLF) band, between 0 and 0.03 Hz; low frequency band (LF), between 0.03 and 0.15 Hz; and high frequency band (HF), between 0.15 and 0.4 Hz. LF and HF bands have been shown to convey information about the ANS control on the heart rhythm, representing the balance between the sympathetic and parasympathetic contributions. Spectral based methods, such as Fourier Transform or Auto-regressive Modeling, require the RR-interval time series to be resampled into a uniform sampling grid.

The analysis of the HRV is often performed on 24 h Holter recordings, and a common procedure is to divide the RR-Intervals time series into 5 min segments, in order to study the evolution of the spectral components along time. Classic techniques for computing the spectrum of HRV signals aim to obtain a good estimate of LF and HF components, but due to the nonuniform sampling and the noisy nature of the measurements, estimating the HRV

Table 5
Mean S/E and (std) for different functions (SNR = 10 dB, Gaussian noise, and $u=T/10$). Two best in bold.

Alg.	CHRP	3SIN	PTR	SAW	FBRK	POL	BPSK	PLST
Yen	11.1 (1.0)	12.5 (0.9)	11.2 (1.0)	6.7 (0.5)	**11.6** (0.9)	13.3 (1.1)	9.3 (0.7)	13.2 (1.1)
Wien	9.6 (1.0)	9.1 (0.9)	9.1 (0.9)	5.1 (0.7)	9.0 (0.9)	9.4 (0.9)	8.5 (0.9)	9.4 (1.0)
Wien-Id	11.3 (1.1)	8.9 (1.3)	**13.4** (1.0)	**7.4** (0.9)	10.7 (1.0)	9.4 (0.4)	10.8 (1.1)	10.0 (0.4)
SVM-Corr	11.0 (1.0)	**13.4** (1.3)	12.2 (1.2)	7.2 (0.6)	11.5 (1.0)	**16.7** (1.4)	**11.6** (0.8)	**15.7** (1.3)
SVM-CorrId	**13.0** (1.1)	**15.2** (1.4)	**14.1** (1.2)	**9.1** (0.9)	**12.9** (1.0)	**18.7** (1.8)	**13.4** (0.9)	**17.5** (1.4)
SVM-RBF	10.7 (0.9)	11.5 (0.9)	10.8 (1.0)	6.8 (0.7)	11.1 (0.9)	14.6 (1.0)	10.0 (0.8)	14.6 (1.3)
SVM-Sinc	**11.3** (0.9)	12.6 (1.0)	10.8 (1.0)	6.6 (0.6)	11.4 (0.9)	13.2 (1.1)	9.3 (0.8)	13.1 (1.2)

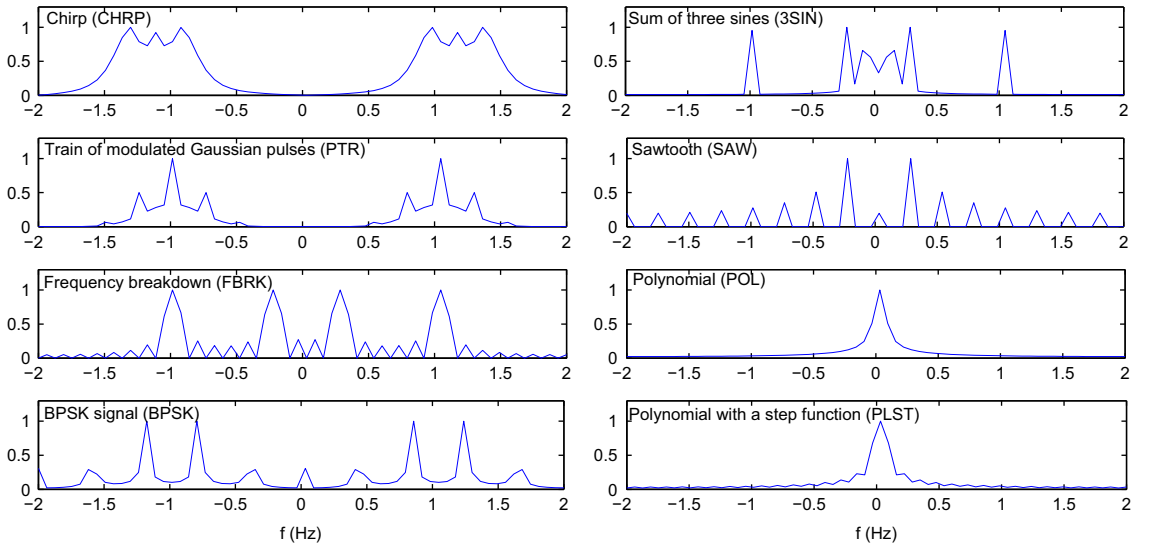

Fig. 7. Spectra of the band-limited signals used for comparing the algorithms. A diversity of spectral profiles has been used for this set of experiments.

spectrum is a very hard problem, specially in LF and HF ranges. In this experiment, we applied the SVM algorithms for interpolating two HRV signals with this purpose.

4.6.2. Methodology

A 24 h Holter recording from a patient with Congestive Heart Failure (labeled with a *D*) and another one from a healthy patient (labeled with an *H*) have been used for this experiment. These recordings were divided into 5-min segments, and two preprocessing steps were done: (1) discarding the segments with more than a 10% of invalid measurements, usually due to low signal amplitude or ectopic origin of the beat; (2) applying a detrending algorithm to subtract the mean value and the constant trend of each segment, which introduces distortion in the VLF region. Two algorithms were compared: SVM-Corr and SVM-RBF. Both algorithms were used to interpolate each segment, by using the RR-intervals in each segment as the training samples, and interpolating the signal over a uniform grid of 500 ms.

The autocorrelation kernel for each patient was estimated as follows: (1) a set of segments (around 20) with low noise and high power in the LF and HF regions were previously selected; (2) an estimate of the autocorrelation of each of these segments was computed by using the method described in Section 3, over a fine grid with a step of 5 ms; and (3) a mean autocorrelation was calculated from this set of estimates, in order to reduce the noise level. A subjective evaluation based on the spectrograms and some examples have been used to compare them.

4.6.3. Results

The autocorrelation kernels and their spectra for both patients *D* and *H* are shown in Fig. 8. Although they are still noisy, note that in patient *D* only one peak is present (probably due to the disease) and both peaks LF and HF are present in patient *H*. Using the SVM-RBF and the SVM-Corr with these kernels we interpolated each segment. The main effect was that SVM-Corr was able to filter the noise in order to highlight the LF and HF peaks better than the RBF algorithm, specially where the density of noise was very high in frequency bands out of the regions of interest, as can be seen in the examples for both patient shown in Fig. 9(a) for patient *D* and Fig. 9(b) for patient *H*. For this last one, two details for a region of interest and for a region with noise are shown in lower plots. In the three examples it can be checked that the SVM-Corr was able to reduce the noise level better than the RBF algorithm.

Fig. 10 shows the spectrograms of the original and interpolated signals. For both patients, LF and HF peaks were clearer with the SVM-Corr than with the SVM-RBF. A short period of the original and estimated signals is shown in Fig. 11, in which two peaks can be identified which correspond to non-ventricular beats or bad measurements. Note that the SVM-Corr algorithm is able to filter this misleading measurements much better than SVM-RBF

5. Discussion and conclusions

This paper presented an SVM framework for nonuniform interpolation based on spectrally adapted Mercer kernels. We first provided a spectral interpretation of the classical Yen interpolator, the Wiener filter, and the SVM interpolation, which motivated us to analyze spectrally adapted kernels for the SVM algorithm. Among them, the actual and estimated kernels can be computed without a significant increase in complexity, though the actual autocorrelation can be determined in advance only in some specific cases (as in the Wiener filter case).

We carried out several experiments in which the spectrally adapted kernels were compared with low-pass kernels and with other techniques. The results showed that the SVM with the autocorrelation kernels outperformed the other methods regardless the spectrum of the

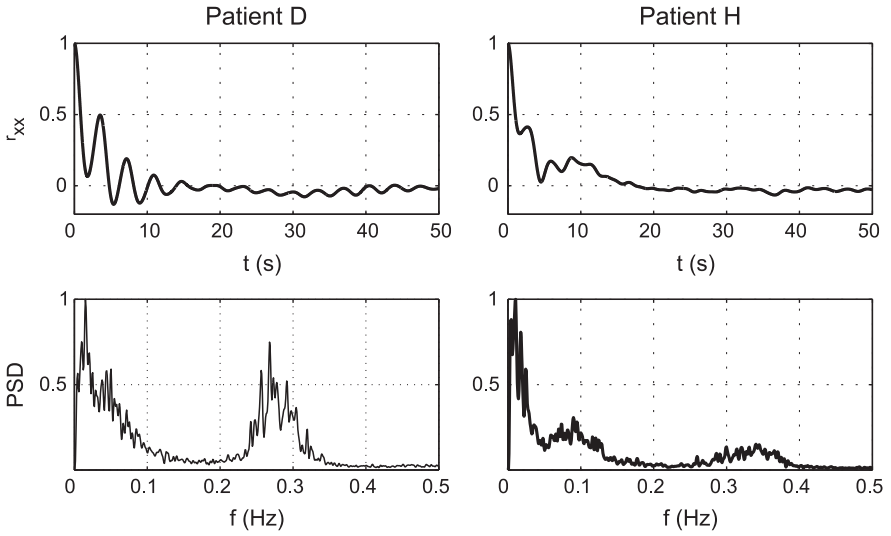

Fig. 8. Autocorrelation kernels in time and frequency for the HRV segments of patients *D* and *H*.

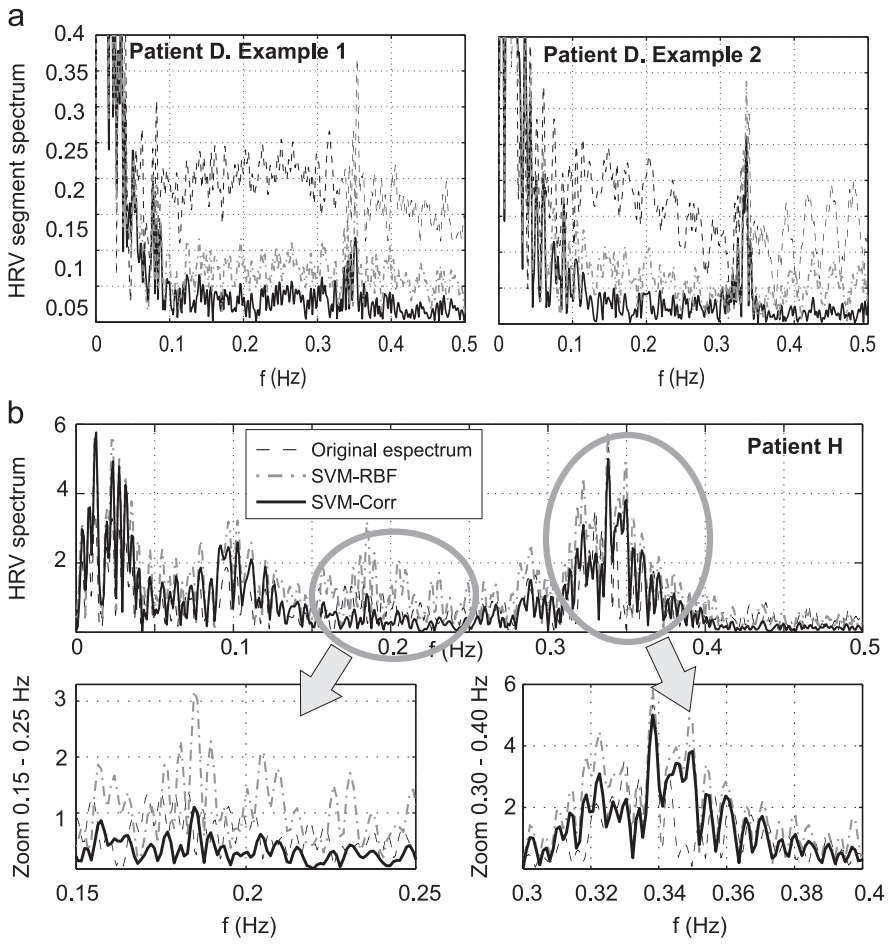

Fig. 9. Examples of HRV segments of patients *D* (a) and *H* (b). Two details of the HRV spectrum for patient *H* are shown in the lower plots.

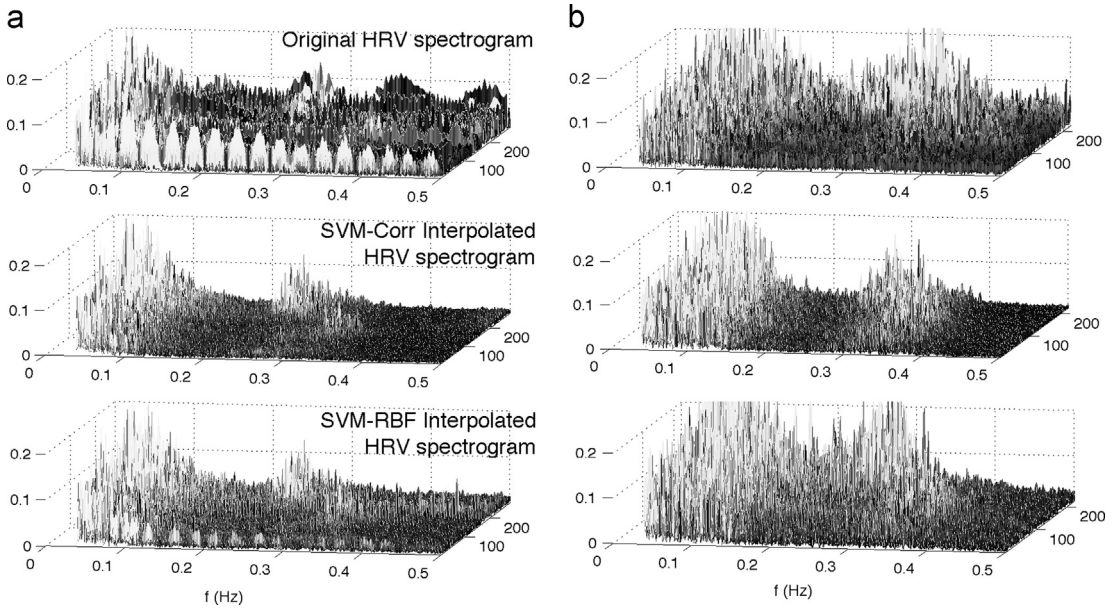

Fig. 10. Spectrograms for the original (upper plot) and reconstructed signals, for patients *D* (a) and *H* (b). Note that noise in intermediate frequencies (0.2–0.25 Hz) is lower in the spectrogram filtered with the SVM-Corr method.

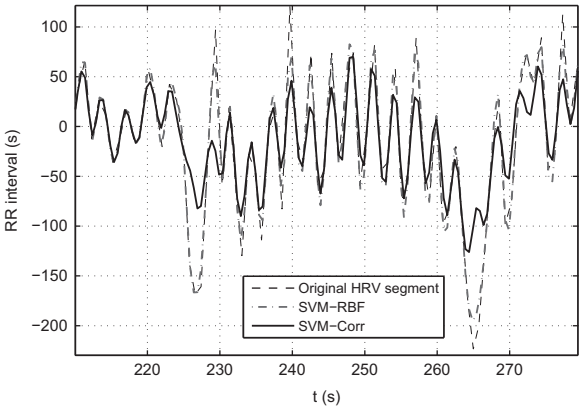

Fig. 11. Example of HRV segment of patient *H* and reconstructed signal with SVM-RBF and SVM-Corr algorithms. Note that the spikes have been filtered with the SVM-Corr algorithm.

observed signal. Also, we also tested the algorithms for several degrees of sampling nonuniformity, for different amount of samples, and for non-Gaussian noise, again concluding that the SVM with the autocorrelation kernels were the most robust method. Finally, we tested the proposed algorithm in a real-life problem, which is the interpolation of HRV signals. In this case, the filtering process carried out with the autocorrelation kernel allowed to attenuate the noise level while enhancing the signal power in the frequency bands of interest.

The proposed method can be especially useful when the signal bandwidth is not known. Also, SVM-based algorithms have shown to provide high performance when the number of available samples is low, which is usual in many interpolation scenarios. With respect to the adjustment of the free parameters, it should be noted that, from a Statistical Learning Theory point of view, there is a training stage in which the signal model is built, but free parameters should be checked to be adequate in a validation set given by a different realization. There is evidence in the literature that SVM interpolation algorithms can be approximately adjusted with free parameters in advance (see [17,25]). Note that the use of autocorrelation kernel avoids tuning the kernel parameters.

In summary, the good properties of SVM algorithms for nonuniform interpolation can be readily improved when a spectrally adapted kernel is used.

Acknowledgments

This work has been partially supported by Research Grants TEC2009-12098 and TEC2010-19263 from Spanish Government, URJC-CM-2010-CET-4482. O.B.P. is supported by FPU grant AP2009-1726.

References

[1] C.E. Shannon, Classic paper: communication in the presence of noise, Proceedings of the IEEE 86 (1998) 447–457.
[2] A. García, Orthogonal sampling formulas: a unified approach, SIAM Reviews 42 (2000) 499–512.
[3] A. Jerri, The Shannon sampling theorem-its various extensions and applications: a tutorial review, Proceedings of the IEEE 65 (1977) 1565–1596.
[4] M. Unser, Sampling-50 years after Shannon, Proceedings of the IEEE 88 (2000) 569–587.
[5] P. Vaidyanathan, Generalizations of the sampling theorem: seven decades after Nyquist, IEEE Transactions on Circuits and Systems I 48 (2001) 1094–1108.
[6] E. Meigering, A chronology of interpolation: from ancient astronomy to modern signal and image processing, Proceedings of the IEEE 90 (2002) 319–342.
[7] T. Strohmer, Numerical analysis of the non-uniform sampling problem, Journal of Computational and Applied Mathematics 122 (2000) 297–316.
[8] H. Choi, D.C. Munson, Direct-Fourier reconstruction in tomography and synthetic aperture radar, International Journal of Imaging Systems and Technology 9 (1998) 1–13.
[9] J.I. Jackson, C.H. Meyer, D.G. Nishimura, A. Macovski, Selection of a convolution function for Fourier inversion using gridding, IEEE Transactions on Medical Imaging 10 (1991) 473–478.
[10] S.M. Kay, Fundamentals of Statistical Signal Processing: Estimation Theory, Prentice Hall, 1993.
[11] J.L. Yen, On nonuniform sampling of bandwidth-limited signals, IRE Transactions on Circuit Theory 3 (1956) 251–257.
[12] E. Diethron, D.C. Munson Jr., A linear time-varying system framework for noniterative discrete-time band-limited signal extrapolation, IEEE Transactions on Signal Processing 39 (1991) 55–68.
[13] G. Kakazu, D.C. Munson Jr., A frequency-domain characterization of interpolation from nonuniformly spaced data, in: IEEE International Symposium on Circuits and Systems, Portland, Oregon, 1989, pp. 288–291.
[14] G. Calvagno, D.C. Munson Jr., New results on Yen's approach to interpolation from nonuniformly spaced samples, in: Proceedings of the IEEE International Conference on Acoustics, Speech, and Signal Processing (ICASSP'90), 1990, pp. 1535–1538.
[15] H. Johansson, P. Löwenborg, Reconstruction of nonuniformly sampled bandlimited signals by means of time-varying discrete-time FIR filters, EURASIP Journal on Advances in Signal Processing 2006 (2006) 1–18.
[16] S. Tertinek, C. Vogel, Reconstruction of nonuniformly sampled bandlimited signals using a differentiator–multiplier cascade, IEEE Transactions on Circuits and Systems I 55 (2008) 2273–2286.
[17] J. Selva, Functionally weighted Lagrange interpolation of band-limited signals from nonuniform samples, IEEE Transactions on Signal Processing 57 (2009) 168–181.
[18] V. Vapnik, The Nature of Statistical Learning Theory, Springer Verlag, 1995.
[19] G. Camps-Valls, J.L. Rojo-Álvarez, M. Martínez-Ramón, Kernel Methods in Bioengineering, Communications and Image Processing, Idea Group, Inc., Hershey, PA, USA, 2006.
[20] J.L. Rojo-Álvarez, C. Figuera-Pozuelo, C.E. Martínez-Cruz, G. Camps-Valls, F. Alonso-Atienza, M. Martínez-Ramón, Nonuniform interpolation of noisy signals using support vector machines, IEEE Transactions on Signal Processing 55 (2007) 4116–4126.
[21] J.L. Rojo-Álvarez, M. Martínez-Ramón, M. de Prado-Cumplido, A. Artes-Rodriguez, A.R. Figueiras-Vidal, Support vector method for robust ARMA system identification, IEEE Transactions on Signal Processing 52 (2004) 155–164.
[22] L. Zhang, W. Zhou, L. Jiao, Wavelet support vector machine, IEEE Transactions on Systems, Man, and Cybernetics, Part B: Cybernetics 34 (2004) 34–39.
[23] C. Figuera, J. L. Rojo-Álvarez, M. Martínez-Ramón, A. Guerrero-Curieses, A.J. Caamaño, Spectrally adapted Mercer kernels for support vector signal interpolation, in: 19th European Signal Processing Conference (EUSIPCO 2011), 2011, pp. 961–965.
[24] N. Wiener, Extrapolation, Interpolation, and Smoothing of Stationary Time Series, Wiley, New York, 1949.
[25] A.J. Smola, B. Schölkopf, A tutorial on support vector regression, Statistics and Computing 4 (2004) 199–222.
[26] J.L. Rojo-Álvarez, G. Camps-Valls, M. Martínez-Ramón, A. Navia-Vázquez, A.R. Figueiras-Vidal, Support vector machines framework for linear signal processing, Signal Processing 85 (2005) 2316–2326.
[27] J.L. Rojo-Álvarez, M. Martínez-Ramón, J. Muñoz-Marí, G. Camps-Valls, C. Martínez Cruz, A. Figueiras-Vidal, Sparse deconvolution using support vector machines, EURASIP Journal on Advances in Signal Processing 2008 (2008) 13.

[28] B. Schölkopf, A.J. Smola, Learning with Kernels, MIT Press, Cambridge, MA, 2001.
[29] P. Laguna, G. Moody, R. Mark, Power spectral density of unevenly sampled data by least-square analysis: performance and application to heart rate signals, IEEE Transactions on Biomedical Engineering 45 (1998) 698–715.
[30] M. Malik, et al., Heart rate variability. Standards of measurement, physiological interpretation, and clinical use. Task Force of the European Society of Cardiology and the North American Society of Pacing and Electrophysiology, European Heart Journal 17 (1996) 354–381.